RESEARCH PAPER

Gut microbial interactions based on network construction and bacterial pairwise cultivation

Min-Zhi Jiang[1], Chang Liu[1], Chang Xu[1], He Jiang[1], Yulin Wang[1*] & Shuang-Jiang Liu[1,2,3*]

[1]State Key Laboratory of Microbial Technology, Shandong University, Qingdao 266000, China;
[2]State Key Laboratory of Microbial Resources, and Environmental Microbiology Research Center (EMRC), Institute of Microbiology, Chinese Academy of Sciences, Beijing 100101, China;
[3]University of Chinese Academy of Sciences, Beijing 100049, China

*Corresponding authors (Shuang-Jiang Liu, meail: liusj@sdu.edu.cn; Yulin Wang, email: wangyulin@sdu.edu.cn)

Association networks are widely applied for the prediction of bacterial interactions in studies of human gut microbiomes. However, the experimental validation of the predicted interactions is challenging due to the complexity of gut microbiomes and the limited number of cultivated bacteria. In this study, we addressed this challenge by integrating *in vitro* time series network (TSN) associations and co-cultivation of TSN taxon pairs. Fecal samples were collected and used for cultivation and enrichment of gut microbiome on YCFA agar plates for 13 days. Enriched cells were harvested for DNA extraction and metagenomic sequencing. A total of 198 metagenome-assembled genomes (MAGs) were recovered. Temporal dynamics of bacteria growing on the YCFA agar were used to infer microbial association networks. To experimentally validate the interactions of taxon pairs in networks, we selected 24 and 19 bacterial strains from this study and from the previously established human gut microbial biobank, respectively, for pairwise co-cultures. The co-culture experiments revealed that most of the interactions between taxa in networks were identified as neutralism (51.67%), followed by commensalism (21.67%), amensalism (18.33%), competition (5%) and exploitation (3.33%). Genome-centric analysis further revealed that the commensal gut bacteria (helpers and beneficiaries) might interact with each other via the exchanges of amino acids with high biosynthetic costs, short-chain fatty acids, and/ or vitamins. We also validated 12 beneficiaries by adding 16 additives into the basic YCFA medium and found that the growth of 66.7% of these strains was significantly promoted. This approach provides new insights into the gut microbiome complexity and microbial inter-actions in association networks. Our work highlights that the positive relationships in gut microbial communities tend to be overestimated, and that amino acids, short-chain fatty acids, and vitamins are contributed to the positive relationships.

human gut microbiome | gut microbial pairwise interaction | co-culture | association network | microbial community

INTRODUCTION

The human gut harbors trillions of bacterial cells, comprising intricate association and interaction networks (Ghoul and Mitri, 2016; Mitri and Foster, 2013). Previous studies have primarily relied on *in silico* co-occurrence or association analyses to discuss microbial relationships in gut microbiome, resulting in a highly descriptive of the field (Bäckhed et al., 2015; Baxter et al., 2019; Coker et al., 2018; Halfvarson et al., 2017; Matchado et al., 2021; Nash et al., 2017; Peng et al., 2018; Qian et al., 2020). It is still a challenge to get a comprehensive insight into bacterial interactions predicted from intertwined association networks. With the growing availability of gut bacterial cultivated resources, it is possible to address the question that how gut microbes associated in networks are interacting with each other.

Inference of microbial association networks is widely applied for mapping microbial interactions (Faust and Raes, 2012; Matchado et al., 2021). Based on the strategies of sampling campaign, microbial association networks could be constructed from longitudinal cohort and cross-sectional cohort studies. Cross-sectional studies provide a "snapshot" of microbial community composition at a specific time point (Odamaki et al., 2016). Correlations between the abundances of different species across individuals do not directly imply interactions, indicating

that longitudinal (time-series) data is likely more suitable for inferring microbial interactions than cross-sectional data (Fisher and Mehta, 2014). In contrast to cross-sectional cohort studies, longitudinal cohort studies enable the investigation of temporal dynamics in microbial communities and inference of local or potentially time-delayed associations (Mars et al., 2020). Ecological interactions between species are intricate, including parasitism, commensalism, mutualism, amensalism, or competition. However, the edges within association networks merely represent positive or negative associations between taxa. It is crucial to note that while association network analysis captures potential links between microbes, these associations are neither necessary nor sufficient to establish ecological interactions (Hsieh et al., 2005). Therefore, experimental methods are important to validate the relationships between taxon pairs within association network.

Compositions of microbial communities were highly dynamic in human gut, resulting in the changed microbial interactions among community members (Palmer and Foster, 2022). The changes of the gut microbial communities were greatly influenced not only by interactions among bacteria but also by hosts and their environments (Hijová et al., 2019; Pan et al., 2022). In terms of microbial community profiling, compared to 16S rRNA gene amplicon sequencing, metagenomic sequencing

is a more suitable approach. In our previous work, we found that microbes from different species share identical 16S rRNA gene V4 or V3/V4 region (Jiang et al., 2022). It could lead to an overestimation of node abundance, thereby increasing its significance within the network. To simplify the complexity of gut microbial community and to overcome the low taxonomic resolution of amplified 16S rRNA gene (V4 or V3/V4 region), we considered that employing *in-vitro* time-series cultivation and shotgun sequencing to predict the association network was highly necessary.

In this study, temporal shotgun metagenomics in combination with co-culture experiment were performed to link the genotype and interaction relationships among microbes in human gut. The primary research objective was to establish a research workflow for predicting and validating the gut microbial interactions *in vitro*. We first performed *in vitro* cultivation with the diluted gut microbiota (10^{-2} and 10^{-4}) on YCFA agar plates. Cultures on plates were then collected in batches of every 2 days (6 time points) for metagenomic shotgun sequencing. We retrieved 198 bacterial metagenome-assembled genomes (MAGs) representing the majority (63.4%) of microbial communities in fecal samples for microbial association network inference. We further isolated the representative strains of taxa in networks and conducted co-culture experiments. Comparative genomic analysis and supplementation culture experiments revealed that the commensalism among phylogenetically closed members of *Clostridia* and *Bacteroidia* in gut microbiome might be dependent on nutrient exchange (e.g., amino acids, vitamins, and short-chain fatty acid (SCFA)).

RESULTS

Profiling fecal microbial communities with metagenomic sequencing

The experimental flow chart is shown in Figure 1A. To characterize the microbial communities in the fecal samples, we sequenced fecal metagenomic DNAs. Meanwhile, in attempt to detect low abundant gut microbes and to extract their interactions with other bacteria, fecal microbial communities were cultivated on YCFA agar plates. The fecal sample was serially diluted in triplicate. Homogenates at two dilution levels (10^{-2} and 10^{-4}) were subsequently plated onto six YCFA agar plates (representing different time points) and incubated under anaerobic and dark conditions at 37°C. Three plates from each dilution were collected every 2 days for metagenomic shotgun sequencing. A total of 419 Gb paired-end reads of high-quality DNA sequences were generated from 36 plates (2 (dilution levels) × 3 (replicates) × 6 (time points)), with approximately 10.6 Gb per cultivated microbial community. Additionally, the donor's fecal sample was sequenced and generated 35.9 Gb DNA sequencing data (Table S1 in Supporting Information). We recovered 198 non-redundant MAGs (Table S2 in Supporting Information), of which 84 MAGs were shared by all samples and 60 MAGs were solely assembled from fecal metagenomic data (Figure 1B). Still, those cultivated microbial communities provided 7 (from 10^{-2}) and 27 (from 10^{-4}) MAGs that were not assembled from the fecal sample metagenome, suggesting the contribution of enrichment for recovering low abundant bacteria. As expected, the MAGs recovered from microbial communities cultivated at lower dilution (10^{-2} group) covered

most of the MAGs from the higher dilution (10^{-4} group). Additionally, the microbial diversity of the 10^{-2} group was higher than that observed within the 10^{-4} group (Figure 1C). The principal coordinate analysis (PCoA) based on Bray-Curtis dissimilarity showed distinct separation of microbial community compositions among cultivated microbial communities with different dilution levels along the PC1 axis (PC1, explained 59.78% of the total variation) (Figure 1D).

Reconstruction of association networks and bacterial growth patterns

To determine the gut microbial associations, we performed an extended local similarity analysis (eLSA) using genome-based relative abundance data of the 10^{-2} and 10^{-4} groups at 6 time points (see Method, Table S3 in Supporting Information, Figure 2A and B). The eLSA analysis provides statistically local similarity and potentially time-delayed association patterns in replicated time series data. As expected, it was found that serial dilution reduced the number of community members and the complexity of microbial association networks. The reconstructed network for the 10^{-2} group included 110 nodes and 496 edges (containing 396 ordinary associations and 100 delayed associations) (Figure 2A; Table S3 in Supporting Information), while the network for the 10^{-4} group included 56 nodes and 143 edges (containing 102 ordinary associations and 41 time-delayed associations) (Figure 2B; Table S3 in Supporting Information). In 10^{-2} and 10^{-4} groups, 12 identical association combinations were predicted, including 7 combinations with consistently predicted associations (positive or negative associations in both groups) (e.g., bin_26-bin_27, bin_81-bin_37, bin_89-bin_102, bin_37-bin_69, bin_79-bin_8, bin_91-bin_99, bin_47-bin_27), and 5 combinations with predicted opposite associations (e.g., bin_101-bin_67, bin_70-bin_60, bin_89-bin_35, bin_23-bin_54, bin_82-bin_69). This suggests that series dilution could not only simplify community composition, but also influence interactions among microbes.

We analyzed the bacterial growth patterns in each dilution group using K-medoids clustering method. In the 10^{-2} dilution group (Figure 2C), three patterns were recognized: Pattern 1 represented microbes (as represented by MAGs) with constantly increasing abundances; Pattern 2 represented microbes (as represented by MAG) with constantly decreasing abundances; and Pattern 3 represented microbes (as represented by MAG) with initial increases followed by decreases. Similar growth patterns were identified for the 10^{-4} dilution cultivation group (Figure 2D). For example, bin_36 (*Christensenella hongkongensis*) and bin_94 (*Parabacteroides distasonis*) exhibited increasing dynamic patterns in biological repeats of 10^{-2} and 10^{-4}, respectively. Then, we considered bin_36 and bin_94 showed a stable growth pattern (Pattern 1) in each of the groups, and we considered them as one of the candidate nodes for validation.

To retrieve the robust associations from the microbial networks, only those nodes of which the corresponding bacteria (as represented by MAG) exhibited consistent growth patterns in all replicates of the specific group (10^{-2} or 10^{-4}) were selected (Table S4 in Supporting Information). After this filtration, 100 MAGs were selected, and they showed 239 associated pairs (either local or time-delayed, Figure 2E and F; Table S5 in Supporting Information) were identified from the association networks. Those MAGs and pairs were applied for guidance of
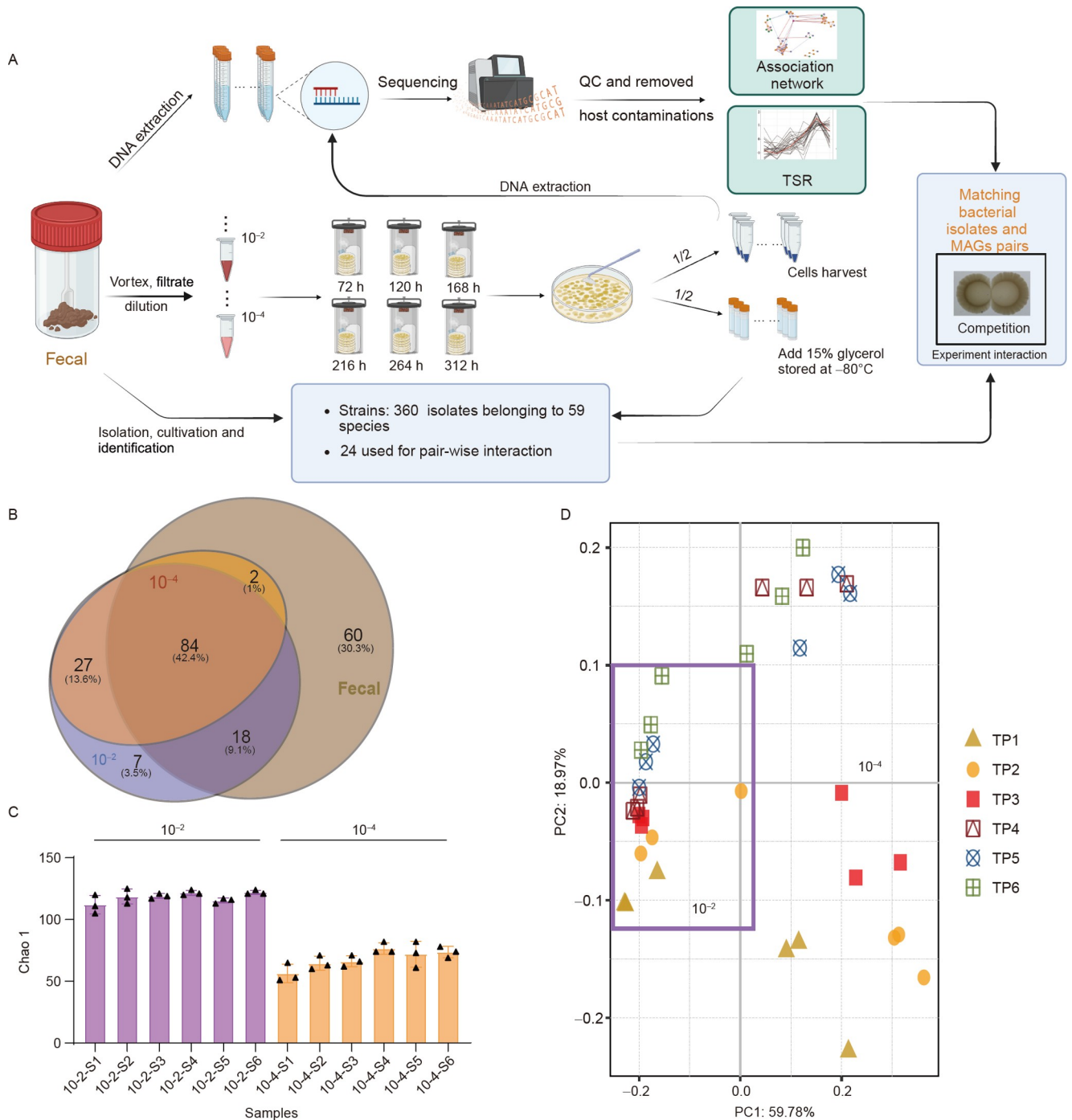
Figure 1. The experimental flow-chart and microbial community comparison. A, Experimental flow-chart. B, Venn diagram showing MAGs recovered from the 10^{-2} and 10^{-4} and fecal samples. C, Microbial diversity of cultivated microbial communities of 10^{-2} (purple group) and 10^{-4} (orange group) determined by Chao 1 index. D, PCoA (Bray-Curtis dissimilarity) of microbial communities. The 10^{-2} group samples were circled into the purple box.

microbial strain isolation and for experimental validation of the predicted microbial interactions from association network analysis.

Bacterial isolation and cultivation

In order to validate the predicted interactions, we made efforts on cultivation and isolation of microbial strains corresponding to the above selected 100 MAGs. A total of 360 isolates representing 35

taxa at genus level were obtained (Figure 3A; Table S6 in Supporting Information). At species level, 24 isolates were matched MAGs of the 100 selected ones (Figure 3B). To obtain further strain resources for testing the predicted interactions from the association network, we searched the human Gut Microbial Biobank (hGMB) (Liu et al., 2021a), and retrieved 19 representative bacterial strains. Thus, we obtained a total 43 microbial isolates/strains representing 43 MAGs out of the 100 selected ones (Figure 3B). With those 43 microbial strains, we would be
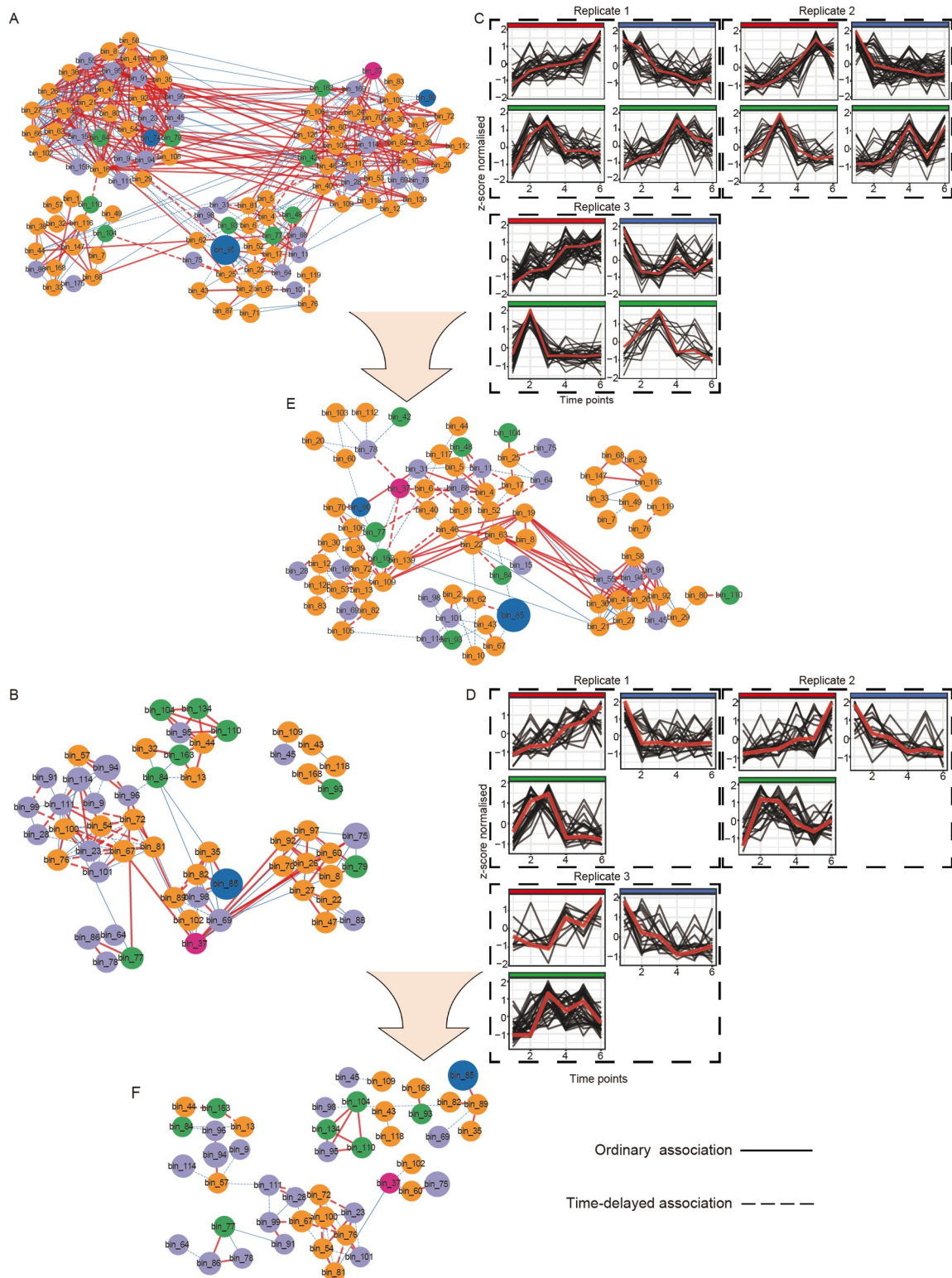
Figure 2. Association network and time series representations (TSR) of gut microbes. For these analyses, MAGs with at least 50% of occurring frequencies in 10^{-2} (A, C, E) or 10^{-4} (B, D, F) dilution cultivation groups were used for plots. A and B, Circle size represents the average relative abundances of MAGs. The dominating phyla are colored, orange for Firmicutes, purple for Bacteroidota, green for Actinobacteria, blue for Proteobacteria, and pink for Desulfobacterota. Red edge represents positive interactions, blue edge represents negative interactions, and the line thickness represents the strength of association. The solid line represents direct associations, and dashed line represents the time-delayed association. C and D, TSR analysis of MAGs abundances using R package Tsrepr. x- and y-axes of these subpanels represent the relative abundance (z-score normalized) of bacteria and sampling time point, respectively. Community members of 10^{-2} and 10^{-4} groups were assigned into 4 and 3 clusters, respectively. The clustering process was independently conducted for each biological replicate (3 replicates for each dilution group), resulting in a total of 12 subpanels (4 clusters × 3 replicates) and 9 subpanels (3 clusters × 3 replicates) in (B) (10^{-2}) and (E) (10^{-4}), respectively. The gray line represents the relative abundance (using z-score normalization) of each MAG changed over time, and the red line representscentroids of patterns. E and F, Filtered sub-networks for experimental validation of the predicted microbial interactions from panels (A) and (B).
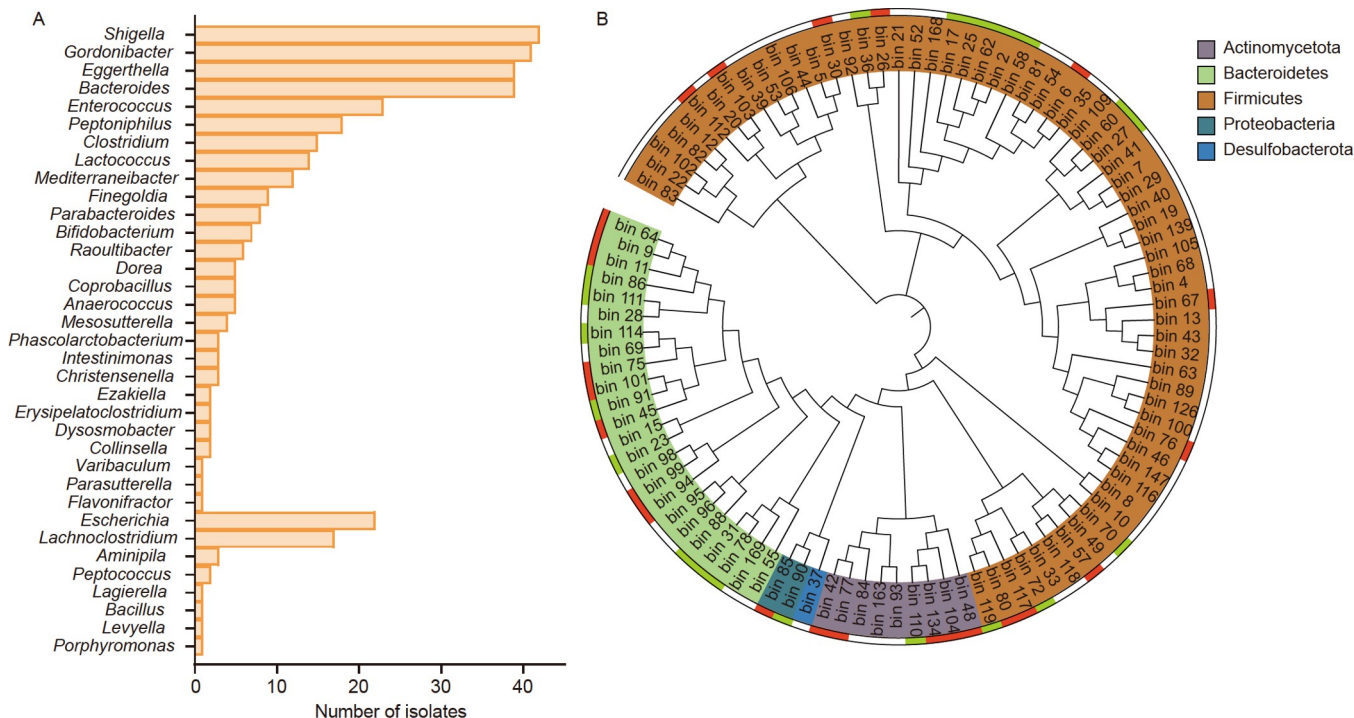
Figure 3. Microbial isolates from this study and taxonomic distribution of the chosen 100 MAGs and corresponding microbial isolates/strains. A, The numbers of isolates at genus level. B, The phylogenetic tree is generated with 120 ubiquitous single-copy marker genes under the WAG model (Parks et al., 2018), and the color blocks of the inner circle indicate phyla. For the outer circle, the green blocks (*n*=19) indicate the strains derived from the hGMB, and red blocks (*n*=24) indicate the strains derived from this study.

able to experimentally test 60 association pairs, including 32 predicted positive and 28 predicted negative associations (Table S7 in Supporting Information).

Co-culture of taxon pairs for validation of predicted associations

Using the cultivated bacterial isolates, we conducted co-culture experiments to validate the microbial interactions of the robust taxon pairs predicted from *in silico* association networks. In total, we identified 60 cultivated bacterial isolate combinations representing 60 taxon pairs in the association network. Subsequently, all 60 cultivated bacterial isolate combinations were co-cultured on YCFA agar plates, and the results (Figure 4) showed the relationships between positively associated taxa could be commensalism, exploitation, amensalism, and neutralism, and relationships between negatively associated taxa could be amensalism, commensalism, competition, exploitation, and neutralism (Figure 5; Table S7 in Supporting Information). Despite the complexity of observed interactions in co-culture experiments, we found that the phenotype of neutralism was identified as the most prevalent relationship (51.67%) between the robust taxon pairs inferred by network analysis (Table S7 in Supporting Information). Specifically, 65.63% and 35.71% of the interactions between taxa with positive and negative associations in networks were identified as neutralism, respectively.

Based on the observed phenotypes, we classified the relationships between the bacterial isolates as profitable (commensalism and exploitation) or competitive (amensalism, competition, and exploitation). The phenotype of profitable interaction showed that at least one isolate could be enhanced. One example for the commensalism phenotype is that *Eggerthella lenta* (bin_77) is

beneficial to *Bacteroides ovatus* (bin_86) as evidenced by the higher density of *Bacteroides ovatus* at the junction of these two bacterial colonies, while the *Eggerthella lenta* does not be affected by *Bacteroides ovatus* (Figure 4B). On the other hand, for the competition phenotype, the growth of *Intestinimonas butyriciproducens* (bin_67) and *Shigella flexneri* (bin_85) were inhibited at the areas close to each other.

When bacterial species have similar environmental preferences or respond to the same external factors and nutrients are not limited, they appear as positive association in their dynamic profile. However, this statistical association does not necessarily mean that they are interacting directly or that their relationship is biologically relevant. We, therefore, assigned the neutral relationship of co-culture experiment as correct confirmation of taxon pairs in networks. By doing so, the agreement rate of the experimental results with the prediction for the 10^{-2} group was 64.29% and that of the prediction for the 10^{-4} group was 72.22%. The agreement rate of the prediction for positive association was 81.82% and 100% in the 10^{-2} and 10^{-4} groups, respectively, while that for negative association was 55% and 37.5% in 10^{-2} and 10^{-4} groups, respectively. Additionally, the final phenotype agreement rate of potentially time-delayed association patterns was 66.67% and 60% in the 10^{-2} and 10^{-4} groups, respectively. In summary, the experimental results fitted largely with the prediction results, and the positive associations in the community were predicted more correctly.

Genome-scale metabolic analysis revealing the nutrient flow within positive taxon pairs

To link the observed phenotypic results to the genotypic relationships, we reconstructed metabolic pathway of the
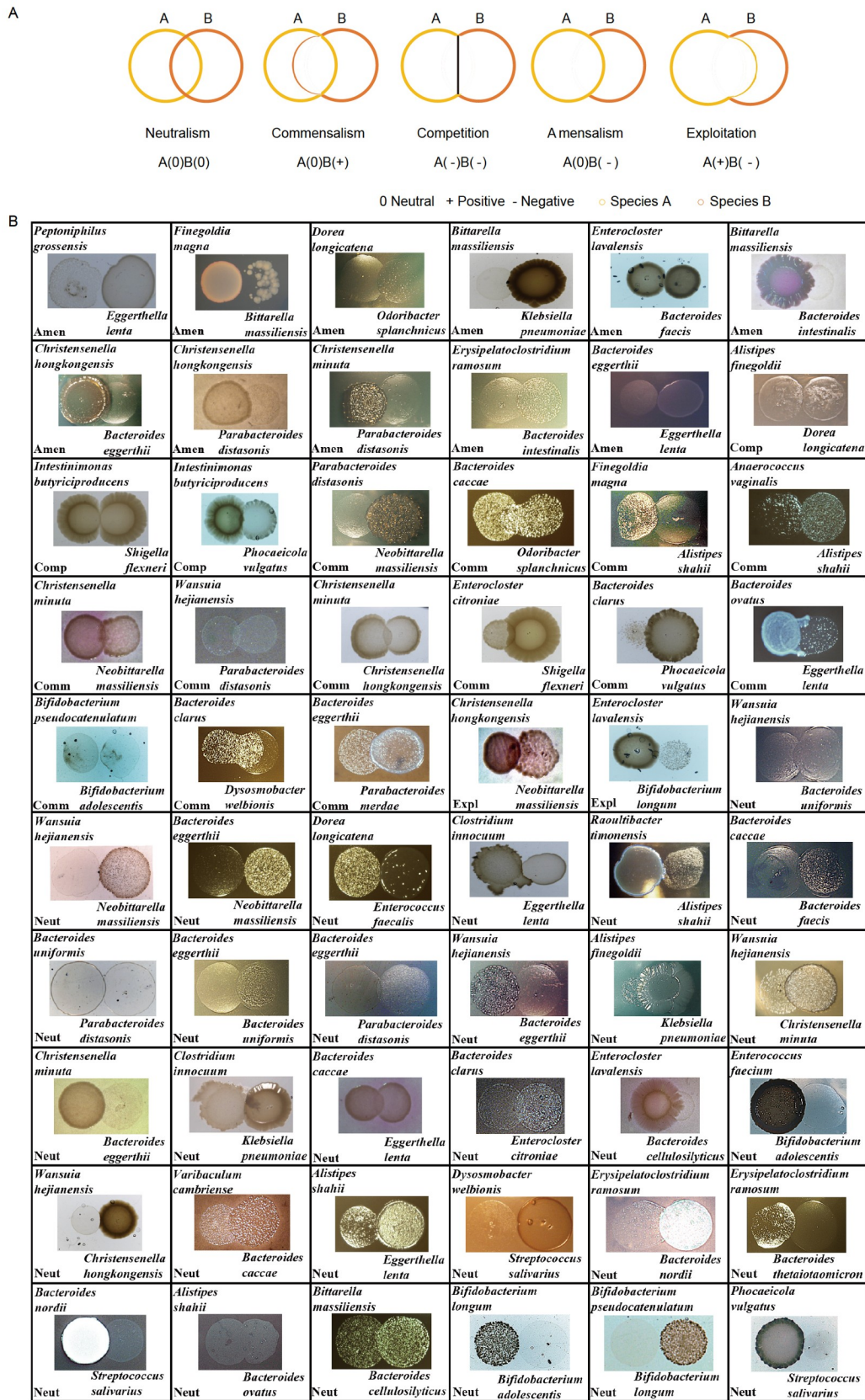
Figure 4. Co-cultivation experiments on YCFA agar plates. A, Schematic diagram illustrating the morphological features of co-cultivated bacteria with different types of associations. B, Interactions of bacterial isolates on YCFA agar plates. For each panel, strain names were labeled at the up-left and bottom-right corners, and their associations were labeled at the bottom-middle with the letter Amensalism (Amen), Commensalism (Comm), Competition (Comp), Exploitation (Expl), or Neutralism (Neut). Photographs were taken after bacterial growth on YCFA agar plates for 4 days at 37°C under anaerobic conditions.
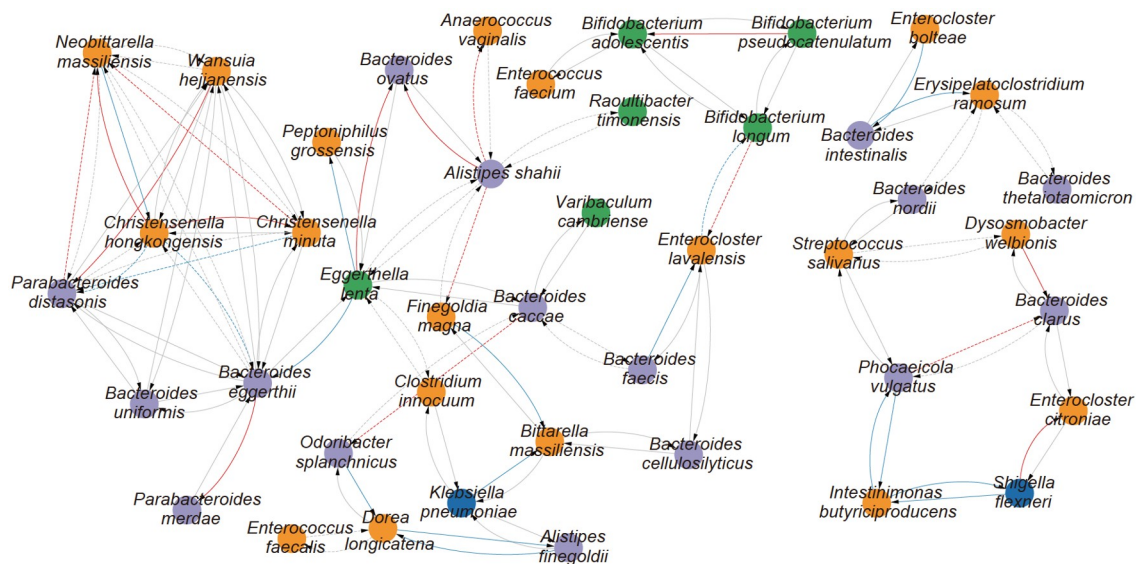
Figure 5. The interaction relationship of cultivated bacterial isolate combinations. Network plots described the interaction relationship of cultivated bacterial isolate combinations. The dominating phyla were colored, orange for Firmicutes, purple for Bacteroidota, green for Actinobacteria, and blue for Proteobacteria. Red edges were positive interactions, blue edges were negative interactions, solid arrows represented the interaction phenotype consistent with the prediction, and dashed arrows represent the interaction phenotype inconsistent with the prediction.

corresponding bacterial MAGs involved in the experimentally studied taxon pairs using EnrichM (v0.6.4) and summarized their KEGG module completeness. Firstly, the results of co-culture experiment were divided into two groups of interactions based on their interaction phenotype: profitable group, including commensalism (0/+), exploitation (−/+); and competitive group, including amensalism (0/−) and competition (−/−) (Table S8 in Supporting Information). We observed that certain microbes in the profitable group acted as "helpers" that promoted the growth of associated microbes (hereafter called "beneficiaries"). Interestingly, the helpers in the profitable group are highly versatile as evidenced by their significantly greater number of metabolic modules than that of beneficiaries (Figure S1 in Supporting Information). However, this difference was not observed in the competitive group (Competitor_A vs. Competitor_B). Besides, the module number in Competitor_A or Competitor_B did not significantly differ from that of helpers in the profitable group.

Furthermore, the incomplete or absent metabolic modules typically found in beneficiaries (>50% of group members) are amino acid biosynthesis (e.g., valine, leucine, isoleucine, lysine, histidine, methionine, tryptophan, ornithine, and arginine), fatty acid biosynthesis (e.g., acetate, propionate, and butyrate), and vitamin biosynthesis (e.g., riboflavin, thiamine, tetrahydrofolate, and cobalamin). Interestingly, we found that beneficiaries were incapable of synthesizing the amino acids with the high metabolic costs, such as tryptophan, methionine, and lysine (Figure 6; Table S8 in Supporting Information). These results suggested that the amino acid, fatty acids, and vitamins were the potential cross-feeding components between helpers and beneficiaries. In summary, the microbes with high metabolic diversity could promote the growth of auxotrophic microbes by providing them amino acids, SCFAs, and vitamins.

Moreover, within the profitable group, it was found that helpers and beneficiaries tended to have a close phylogenetic relationship, and this relationship could even be observed at a relatively higher taxonomic level (e.g., class level) (e.g., Clostridia

and Bacteroidia) (Table S7 and Figure S2 in Supporting Information). Specifically, 46.67% of taxon pairs of the validated profitable group were found to be affiliated with the same order, suggesting that kin selection might determine the gut microbial community assembly (Harcombe, 2010). However, this trend was not observed in the competitive group. Members within the taxon pairs of competitive groups showed high taxonomic divergence as none of them were from the same bacterial orders.

We introduced 16 nutrient additives (see Methods) into YCFA medium, and monitored the growth curves of these beneficiaries (Figure S3 in Supporting Information) for 48 h (normalized with the first time point). Our findings revealed that additives could enhance the maximum biomass for most microbials (66.67%), such as *Bacteroides ovatus*, *Bacteroides clarus*, *Bifidobacterium adolescentis*, *Enterocloster lavalensis*, *Neobittarella massiliensis*, *Odoribacter splanchnicus*, *Parabacteroides distasonis*, and *Parabacteroides merdae*. However, *Enterocloster citroniae* experienced a reduction in their maximum biomass. The additives had no impact on the growth status of the three microbes, including *Anaerococcus vaginalis*, *Christensenella minuta*, and *Finegoldia magna* (Figure 7). Additionally, additives not only enhanced the maximum biomass of microbes but also significantly reduced their generation time, as observed with *Christensenella minuta*, *Enterocloster citroniae*, *Enterocloster lavalensis*, and *Parabacteroides merdae*. Additives increased the maximum biomass of *Bacteroides ovatus* while increasing its generation time (Figure S4 in Supporting Information).

DISCUSSION

The aim of this study was to establish a workflow based on cultivation that could serve as a platform for predicting and investigating bacterial interactions between at species or strain level. The *in vitro* cultivation in the present study was conducted using YCFA, a commonly used medium for isolating and cultivating intestinal microbes (Browne et al., 2016; Duncan et
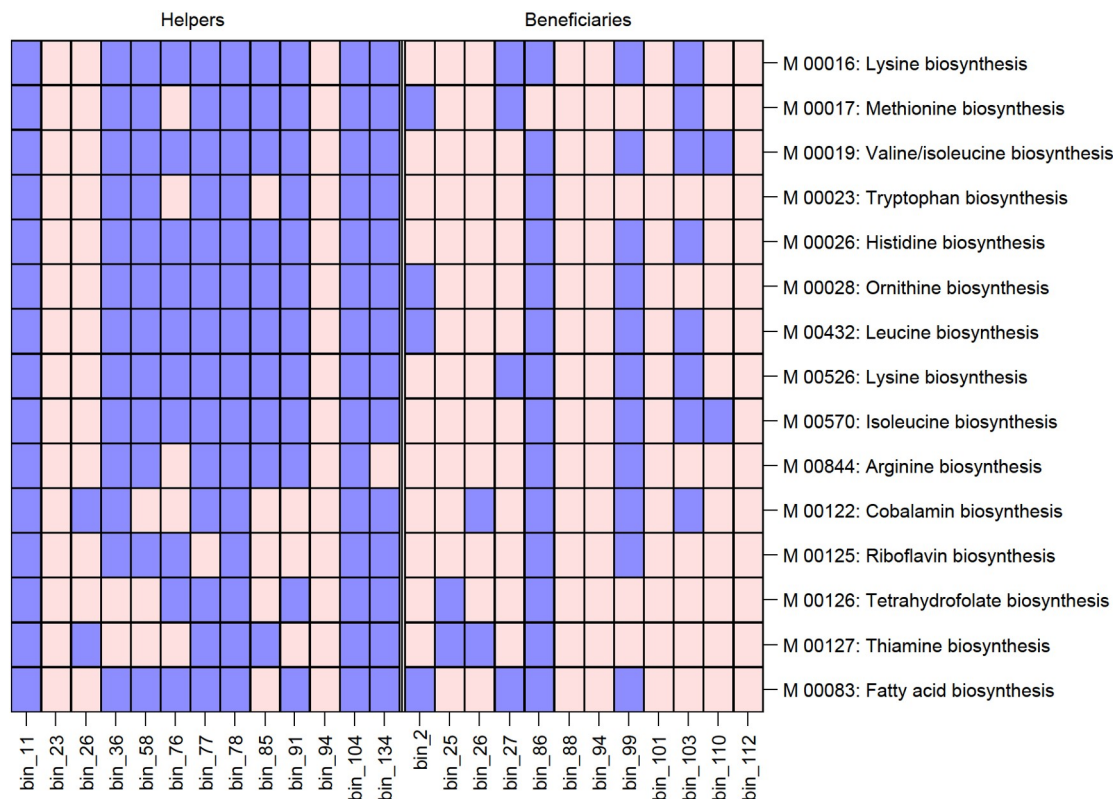
Figure 6. Complete and incomplete metabolic modules in helpers and beneficiaries. The purple blocks represent complete metabolic modules in each MAG, and the pink blocks represent incomplete metabolic modules in each MAG.
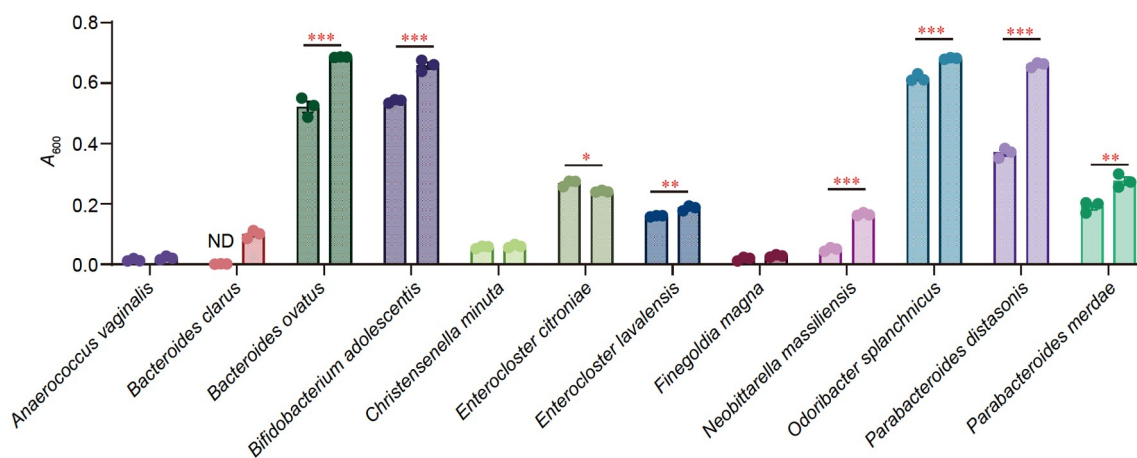
Figure 7. Evaluating the biomass (as indicated with A_{600}) of each beneficiary under different culture conditions. In the bar chart, the left column of each beneficiary represented the microbe cultured into YCFA base medium, and the right column of each beneficiary represented the microbe cultured into YCFA supplementation medium. (*t*-test, $P<0.05$). Data were shown as the mean±SEM. The P value was calculated by two-sided paired *t*-test (*, $P<0.05$; **, $P<0.01$; ***, $P<0.001$).

al., 2002; Forster et al., 2019; Lagkouvardos et al., 2017). The culture media used for growing or enriching would impact on bacterial growth and diversity. Yuan et al. (2023) recently reported that the growth matrix modulated plant microbiome and the modulated microbiome further impacted insect behavior. This reminds us that food intake, human immunity and physiology would modulate gut microbiome interactions, which would extremely complicate the microbial interactions in host guts.

Association network analysis based on time series metage-

nomics has been frequently used to infer microbial relations in environmental or host-associated microbiomes, including the gut microbiome (La Fata et al., 2018). Although microbial association networks are readily available, still, the identification of true microbial interactions is challenging and is an important step towards understanding the gut microbial community assembly. This necessitates a high throughput experimental method to validate the microbial interactions inferred from *in-silico* analyses. However, the high microbial diversity and unstable conditions are limiting factors for the understanding of organ-

ism's interactions in human gut (Fan and Pedersen, 2021). To address this challenge, we present a strategy to simplify the gut microbial community and *in vitro* time course cultivation on YCFA agar medium, which is of great importance in the identification of reliable interactions between gut microbial species. *In vitro* cultivated time series samples could effectively avoid interference from the host gut immune system, and the community behavior can be predictable.

One hurdle in conducting co-culture experiments is cultivation of "uncultivable" microbes. We found that 63.4% of indigenous microbes could be identified on YCFA plates, confirming the effectiveness of the YCFA medium in cultivating most human gut microbes (Browne et al., 2016; Duncan et al., 2002; Forster et al., 2019; Lagkouvardos et al., 2017). This also provides the basis for inferring representative microbial association networks of the human gut using *in-vitro* culturing experiments. Since both the microbial association networks and bacterial isolates were obtained from the *in-vitro* cultivation experiment, bacterial strains isolated from the YCFA medium could be directly linked to the taxon nodes in the microbial association networks. The bacterial isolates obtained from the present study in combination with the existing isolates in hGMB covered approximately 25.1% of robust taxon pairs in microbial association networks.

Co-culture experiment conducted in a controlled environment has been widely applied to verify microbial interactions (Liu et al., 2021b; Venturelli et al., 2018; Weiss et al., 2022). Previous studies have demonstrated the consistent results between the statistical associations inferred from cross-sectional or longitudinal cohorts and validating experiments conducted *in vitro* (Clavel et al., 2006; Kanazawa et al., 2021; Liu et al., 2022; Lohia et al., 2022; Petrov et al., 2017; Ruaud et al., 2020). These studies suggest that *in vitro* co-culture experiments are relevant for inferring how bacteria interact in vivo. It is worth noting that the majority of (65.63%) positively associated taxon pairs in the microbial association networks have been experimentally confirmed as neutral, suggesting that cooperation between two species is typically rare (Palmer and Foster, 2022). This inconsistent result may primarily stem from the inherent limitations of inferring ecological inter-species interactions directly from sequence data and statistical association analysis. It is important to keep in mind that species abundances can exhibit significant variations over time, and these nonlinear dynamics commonly lead to ephemeral associations over certain time window or at certain state (Sugihara et al., 2012). Therefore, statistical association networks can hardly distinguish between ecological interactions and other nonrandom processes (e.g., niche overlap). Moreover, our finding suggested that the *in-silico* analyses are inadequate to explore the real interactions between gut microbes. In the present study, we relied on pairwise co-culture experiments to validate the ecological interactions of taxon pairs within the association networks. While this approach may hardly capture the complex communal behaviors, it can validate a subset of bacterial interactions under controlled condition. Considering that the statistical associations in a complex community might be due to many mediator species and external factors, experiments of systems-level community dynamics should be taken into consideration in future studies.

We examined the phenotypes of validated positive and negative interactions among microbes. Owing to the time series shotgun metagenomic sequencing, we could investigate the genome-scale metabolic models among the validated interac-

tions. Our reconstructed metabolic models highlighted that the exchange of amino acids, SCFAs, and vitamins played a significant role in the development of positive associated microbe relationships in the human gut. One commensalism relationship between *Bacteroides ovatus* and *Eggerthella lenta* was experimentally confirmed by a previously reported study, which found that the primary cross-feeding components were amino acids (e.g., phenylalanine, valine, gamma-glutamylisoleucine) (Venturelli et al., 2018). We attempted to evaluate the effects of amino acids, SCFAs, and vitamins on the growth of beneficiaries by adding them to YCFA medium. We found that 66.7% of the experimental groups showed an enhancement in growth. Microbes that did not exhibit noticeable changes in growth may be due to the absence of certain unidentified growth factors in the medium, possibly because the incompleteness of the genome for metabolic pathway prediction. We also inferred that the competition relationship might improve the colonization resistance in the gut. For instance, *Shigella flexneri*, an opportunistic pathogen, could cause a gut infection known as shigellosis, with more than 160 million cases of shigellosis occurring worldwide each year (Macmicking, 2017). We found that *Intestinimonas butyriciproducens* (bin_67) could inhibit the growth of *Shigella flexneri* (bin_85) by competition.

In addition to the direct microbial interactions, it is worth noting that the high-order interaction might play an important role in community assembly and stability. While this high-order interaction can be hardly tested by co-culture experiment, we could attempt to infer the indirect relationships between microbes if one microbe involved in multiple taxon pairs. Prediction of this kind of high-order interactions may provide new insights into the gut microbial community assembly and play a critical role in regulating the community composition and function. For instance, the inferred relationship between bin_101-bin_23 was strong negative interaction, but the co-culture experiment of the representative isolates (*Bacteroides clarus-Phocaeicola vulgatus*) was commensalism. Remarkably, we identified isolates from two strains, *Intestinimonas butyriciproducens* (bin_67) and *Phocaeicola vulgatus* (bin_23), that showed a competition relationship when the isolates were closed. We speculated that *Intestinimonas butyriciproducens* (bin_67) could inhibit the growth of *Phocaeicola vulgatus* (bin_23), and *Phocaeicola vulgatus* (bin_23) could enhance the growth of *Bacteroides clarus* (bin_101) leading to the strong negative interaction between *Bacteroides clarus* (bin_101) and *Phocaeicola vulgatus* (bin_23).

In vitro pairwise co-culturing can validate a subset of gut microbial associations, as microbes from given lineage could not be cultivated by YCFA medium. Despite having a high relative abundance in the fecal sample (>2%), some gut microbes (e.g., bin_113, bin_124, bin_131, bin_153, bin_154, bin_164, bin_166, bin_176, bin_183, bin_193) from *Firmicutes* could not be cultivated by YCFA agar medium. Additional modified cultural conditions besides YCFA could increase the diversity of the cultivable microbes. For example, the modified mGAM medium with extra addition of carbohydrate mixture has been demonstrated to significantly increase the biodiversity on agar plates (Liu et al., 2021a). For future studies, we need to construct voluminous interaction networks using comprehensiveness isolates collection obtained from a larger number of fecal samples and modified cultural conditions. Also, future studies should incorporate enumeration methods to validate higher-order

interactions of gut microbe communities.

MATERIALS AND METHODS

Fecal sample collection and cultivation/extraction of gut microbiomes

The whole project was approved by the Research Ethics Committee of the Institute of Microbiology, Chinese Academy of Science, and the assigned number authority of the ethical approval is APIMCAS2017049. Fecal samples were collected from a healthy female from China who had not taken antibiotics within the last 3 months (Additional file 1 in Supporting Information). The samples were kept fresh and transferred into an anaerobic workstation (Coy Laboratory Products Inc., USA). The gas flow composition in the anaerobic workstation was 85% (N_2), 5% (CO_2), and 10% (H_2). Fecal samples were homogenized in sterilized PBS solution containing NaCl 136 mmol L^{-1}, Na$_2$HPO$_4$ 8 mmol L^{-1}, KH$_2$PO$_4$ 2 mmol L^{-1}, KCl 2.6 mmol L^{-1}, L-Cysteine 4 mmol L^{-1} at pH 7.4, with a ratio of 1 g stool per 1 mL PBS. The homogenate was filtered using a 40 μm cell strainer (BD Falcon, USA) and equally divided into three 1.5 mL tubes. The serial dilution was conducted in triplicate (fecal sample (FS)-1, -2, and -3). The dilutions 10^{-2} and 10^{-4} were plated directly onto YCFA agar respectively, named 10^{-2}-FS1, -FS2, -FS3 (10^{-2} group) and 10^{-4}-FS1, -FS2, -FS3 (10^{-4} group) in sextuplicate (6 time points for temporal collection). A total of 36 YCFA plates (2 (dilution level) × 3 (triplicate) × 6 (time points)) were inoculated at anaerobic and dark conditions and at 37°C. One plate from each fecal sample (FS1, FS2, and FS3) was collected at 72, 120, 168, 216, 264 and 312 h, resulting in 3 plates for each group (10^{-2} and 10^{-4}) at given sampling point. Biomass collected from the same dilution rate at the same time point was harvested. Half of the biomass was resuspended using 1 mL 15% glycerol and stored at −80°C until use.

Metagenomic sequencing, assembly and genome annotation

The fecal samples (1 sample) and harvest biomass from plates (36 samples) were subjected to DNA extraction and purification using DNeasy PowerSoil Kit (Qiagen, Germany). Paired-end libraries were constructed and sequenced on Illumina Novaseq 6000 platform to generate 150 bp paired-end reads with a 350 bp insert size by Novogene Technology Co., Ltd., (Beijing, China). The raw data were trimmed by SOAPnuke (v2.1.7) (Chen et al., 2018) and were subsequently aligned to the *Homo sapiens* (GCF_000001405.39) reference genome to remove the host contamination using bowtie2 (v2.3.5.1) (Langmead and Salzberg, 2012). The clean reads were *de-novo* assembled using SPAdes (v3.13.0) (Bankevich et al., 2012) with the default parameters. Contigs≥1,500 bp were used for binning with MetaWRAP (v1.3.2) (Uritskiy et al., 2018). MAGs with completeness≥50% and contamination≤10% were used for subsequent analysis. The set of quality-filtered MAGs was dereplicated using dRep (v2.2, nc 0.6 ANI 99) (Olm et al., 2017). A total of 198 non-redundant bacterial MAGs were retained. The MAGs were classified with GTDB-TK (v1.5.1) based on the Genome Taxonomy Database (release 95) (Chaumeil et al., 2020). The phylogenetic tree was inferred from concatenated alignment of 120 bacterial marker genes from the non-

redundant MAGs and the selected reference genomes under the WAG model (Parks et al., 2018). Gene prediction and annotation of the non-redundant MAGs were performed using Prokka (v1.13) (Seemann, 2014). Metabolic reconstruction of these MAGs was performed using EnrichM (v0.6.4) (https://github.com/geronimp/enrich). KEGG module completeness was defined as the proportion of Steps_found in Steps_needed. To assess the presence of modules in bacterial genomes, we set a threshold of 70%. If the module completeness was >70%, we considered the module as complete in the genome (Johnson et al., 2021; Zimmermann et al., 2021).

Microbial association networks construction and time series representations analysis

The relative abundance of each MAG was estimated using coverM (v0.6.1) (github.com/wwood/CoverM) with "--min-read-percent-identity" 0.9 and "--min-read-aligned-percent" 0.7. MAGs which were detected in less than 50% of the samples in each group (i.e., dilution rate 10^{-2} and 10^{-4}) were filtered before association network construction. Moreover, the relative abundance outlier for biological triplicates was eliminated using R (v3.6.2) (https://www.r-project.org/) package "outliers" (v0.15). Microbial association networks were inferred using eLSA (Xia et al., 2011) with the parameters of -r 3 (three replicates), -s 6 (six time points), and -d 2 (including time-shifted associations of two time points). The inferred association networks were visualized with Cytoscape (v3.9.0) (Cline et al., 2007). Bacterial pairs (MAG pairs) exhibit robust (|local similarity score|>0.6, |ρ|>0.6, *P*<0.05) local associations and time-delayed associations were filtered for the downstream analysis. For the microbial community of each biological replicate, we conducted time series representations (TSR) analysis using R package "Tsrepr" (v.1.1.0) to cluster bacteria with similar temporal dynamic features. We applied K-medoids clustering method to categorize bacteria exhibiting similar dynamic patterns into clusters. Davies-Bouldin index was used to evaluate the optimal number of clusters (*K*). The range of *K* was set between 2 and 10. The community members of 10^{-2} and 10^{-4} groups were assigned to 4 and 3 clusters, respectively. Bacteria clustered into consistent dynamic pattern (e.g., sustained increase or sustained decrease) across biological replicates were deemed to exhibit strong dynamic reproducibility. If both members of a robust association were classified as highly reproducible bacteria, the taxon association would be selected for validation through interaction experiments.

Bacterial isolation and cultivation

Bacterial isolation was performed using two types of samples: fecal samples and cells scraped from the surface of YCFA agar mediums (from the same sample donor). For the fecal sample, insoluble particles were removed by filtration using a 40 μm cell strainer (BD Falcon, USA), followed by serial dilution ranging from 10^{-1} to 10^{-5} using PBS. Glycerol-stored samples, scraped from the surface of YCFA agar mediums, were diluted directly under the same conditions. Subsequently, 50 μL aliquots of the diluted samples were spread onto YCFA (Poyet et al., 2019) or mGAM (Liu et al., 2021a) agar plates and incubated for 5–20 days. Single colonies were then picked from the agar plates, and their purity was confirmed by sequencing their 16S rRNA gene,

following the method described in our previous study ([Liu et al., 2020](#)). Taxonomic classification of the isolates was performed by comparing their 16S rRNA gene sequences against NCBI database with a sequence identity cutoff of 98.7%. Taxonomic assignment of MAGs was analyzed using GTDB-Tk ([Chaumeil et al., 2020](#)). An isolate was assigned as a representative bacterium of a given MAG if it belonged to the same bacterial species.

Pairwise co-culture with representative bacterial isolates

To validate the interactions between MAG pairs in network, representative isolates were cultivated on YCFA agar plates. Monocultures of the representative bacterial isolates were prepared in 5 mL mGAM medium with 1% (v/v=1:1) inoculation and cultured at 37°C for 3–4 days. The growing cells were harvested at 3,000 r min⁻¹ at 4°C for 30 min and resuspended in 0.2 mL YCFA medium. For experimental validation of microbial interactions inferred by the network, the bacterial isolates representing the associated MAGs were co-cultured on YCFA agar plate. Specifically, 3 μL of the representative bacterial isolate cultures were dripped onto the YCFA agar plate surface, followed by the addition of 3 μL of another representative bacterial isolate at external tangency to the first representative isolate. The plates were then cultivated at 37°C for 5 days, and photographs were recorded. According to the pairwise interaction result, we could identify the interaction relationship of pairwise cultivated bacterial strains, including neutralism (0/0), commensalism (0/+), exploitation (−/+), amensalism (0/−) and competition (−/−). Then, we could visualize the validated interaction relationship by using Cytoscape (v3.9.0) ([Cline et al., 2007](#)).

Validation of metabolic interactions of beneficiaries

We defined the microbes within profitable relationship (commensalism, exploitation) that could facilitate the growth of other microbe ("beneficiaries) as "helpers", and we defined the microbes in competitive relationship (competition and amensalism) as "competitor_A" and "competitor_B". Module prevalence was determined as the proportion of complete modules within helpers, beneficiaries, competitor_A or competitor_B MAGs. If the prevalence>50%, We established a control group and experimental groups for this study. The control group was cultured in YCFA medium without any additives, while the experimental groups were added with 16 additives, including 9 amino acids (valine, leucine, isoleucine, lysine, histidine, methionine, tryptophan, ornithine and arginine) (100 mg L⁻¹ respectively, pH 7.3), 4 vitamins (riboflavin, thiamine, tetrahydrofolate, and cobalamin) (0.5, 0.5, 0.5, and 0.01 mg L⁻¹ respectively, pH 7.3) and 3 SCFAs (acetate, propionate, and butyrate) (100 mg L⁻¹ respectively, pH 7.3). Subsequently, the mixed YCFA medium was added into a 96-well plate at a volume of 150 μL per well. Monocultures of the beneficiaries were prepared in 5 mL mGAM medium with 1% (v/v=1:1) inoculation and cultured at 37°C for 3–4 days. The growing cells were harvested at 6,000 r min⁻¹ at room temperature for 5 min and then the supernatant was removed. The pellet was resuspended in YCFA medium, and the optical density (A_{600}) was adjusted to 0.5. Inoculated the adjusted bacterial culture with 1% (v/v=1:1) into a 96-well plate, with three replicates for each sample and measured the A_{600} absorbance every 30 min with a microplate reader (SPECTROstar Omega, Germany). The generation time of each beneficiary was calculated as

$$Gt \text{ (hour/generation)} = (t2 - t1) / \log_2(N2 / N1),$$

where Gt represented the generation time, $t1$ represented the starting time of the logarithmic growth phase, $t2$ represented the ending time of the logarithmic growth phase, $N1$ represented the A_{600} at the starting time of the logarithmic growth phase, $N2$ represented the A_{600} at the ending time of the logarithmic growth phase.

Statistical analysis

All the data are indicated as the means±SEM. GraphPad Prism 9.0 software and Adobe Illustrator 2019 for data analysis and figures modification. The normal distribution was assessed with the Shapiro-Wilk test. Data were shown as the mean±SEM. The P value was calculated by two-tailed unpaired Student's t-test (*, $P<0.05$; **, $P<0.01$; ***, $P<0.001$).

Availability of data and materials

The reconstructed metagenome-assembled genomes in the present study have been deposited in China National Microbiology Data Center (NMDC) with accession numbers NMDC10018525.

References

Bäckhed, F., Roswall, J., Peng, Y., Feng, Q., Jia, H., Kovatcheva-Datchary, P., Li, Y., Xia, Y., Xie, H., Zhong, H., et al. (2015). Dynamics and stabilization of the human gut microbiome during the first year of life. Cell Host Microbe 17, 852.

Bankevich, A., Nurk, S., Antipov, D., Gurevich, A.A., Dvorkin, M., Kulikov, A.S., Lesin, V.M., Nikolenko, S.I., Pham, S., Prjibelski, A.D., et al. (2012). SPAdes: a new genome assembly algorithm and its applications to single-cell sequencing. J Comput Biol 19, 455–477.

Baxter, N.T., Schmidt, A.W., Venkataraman, A., Kim, K.S., Waldron, C., and Schmidt, T.M. (2019). Dynamics of human gut microbiota and short-chain fatty acids in response to dietary interventions with three fermentable fibers. mBio 10, e02566-02518.

Browne, H.P., Forster, S.C., Anonye, B.O., Kumar, N., Neville, B.A., Stares, M.D., Goulding, D., and Lawley, T.D. (2016). Culturing of 'unculturable' human microbiota reveals novel taxa and extensive sporulation. Nature 533, 543–546.

Chaumeil, P.A., Mussig, A.J., Hugenholtz, P., and Parks, D.H. (2020). GTDB-Tk: a toolkit to classify genomes with the Genome Taxonomy Database. Bioinformatics 36, 1925–1927.

Chen, Y., Chen, Y., Shi, C., Huang, Z., Zhang, Y., Li, S., Li, Y., Ye, J., Yu, C., Li, Z., et al. (2018). SOAPnuke: a MapReduce acceleration-supported software for integrated quality control and preprocessing of high-throughput sequencing data. Gigascience 7, 1–6.

Clavel, T., Henderson, G., Engst, W., Doré, J., and Blaut, M. (2006). Phylogeny of human intestinal bacteria that activate the dietary lignan secoisolariciresinol diglucoside. FEMS Microbiol Ecol 55, 471–478.

Cline, M.S., Smoot, M., Cerami, E., Kuchinsky, A., Landys, N., Workman, C., Christmas, R., Avila-Campilo, I., Creech, M., Gross, B., et al. (2007). Integration of biological networks and gene expression data using Cytoscape. Nat Protoc 2, 2366–2382.

Coker, O.O., Dai, Z., Nie, Y., Zhao, G., Cao, L., Nakatsu, G., Wu, W.K., Wong, S.H., Chen, Z., Sung, J.J.Y., et al. (2018). Mucosal microbiome dysbiosis in gastric carcinogenesis. Gut 67, 1024–1032.

Duncan, S.H., Hold, G.L., Harmsen, H.J.M., Stewart, C.S., and Flint, H.J. (2002). Growth requirements and fermentation products of *Fusobacterium prausnitzii*, and a proposal to reclassify it as *Faecalibacterium prausnitzii* gen. nov., comb. nov. Int J Syst Evol Microbiol 52, 2141–2146.

Fan, Y., and Pedersen, O. (2021). Gut microbiota in human metabolic health and disease. Nat Rev Microbiol 19, 55–71.

Faust, K., and Raes, J. (2012). Microbial interactions: from networks to models. Nat Rev Microbiol 10, 538–550.

Fisher, C.K., and Mehta, P. (2014). Identifying keystone species in the human gut microbiome from metagenomic timeseries using sparse linear regression. PLoS ONE 9, e102451arXiv: 1402.0511..

Forster, S.C., Kumar, N., Anonye, B.O., Almeida, A., Viciani, E., Stares, M.D., Dunn, M., Mkandawire, T.T., Zhu, A., Shao, Y., et al. (2019). A human gut bacterial genome and culture collection for improved metagenomic analyses. Nat Biotechnol 37, 186–192.

Ghoul, M., and Mitri, S. (2016). The ecology and evolution of microbial competition. Trends Microbiol 24, 833–845.

Halfvarson, J., Brislawn, C.J., Lamendella, R., Vázquez-Baeza, Y., Walters, W.A., Bramer, L.M., D'Amato, M., Bonfiglio, F., McDonald, D., Gonzalez, A., et al. (2017). Dynamics of the human gut microbiome in inflammatory bowel disease. Nat Microbiol 2, 17004.

Harcombe, W. (2010). Novel cooperation experimentally evolved between species. Evolution 64, 2166–2172.

Hijová, E., Bertková, I., and Štofilová, J. (2019). Dietary fibre as prebiotics in nutrition. Cent Eur J Public Health 27, 251–255.

Hsieh, C.H., Glaser, S.M., Lucas, A.J., and Sugihara, G. (2005). Distinguishing random environmental fluctuations from ecological catastrophes for the North Pacific Ocean. Nature 435, 336–340.

Jiang, M.Z., Zhu, H.Z., Zhou, N., Liu, C., Jiang, C.Y., Wang, Y., and Liu, S.J. (2022). Droplet microfluidics-based high-throughput bacterial cultivation for validation of taxon pairs in microbial co-occurrence networks. Sci Rep 12, 18145.

Johnson, M.D., Scott, J.J., Leray, M., Lucey, N., Bravo, L.M.R., Wied, W.L., and Altieri, A.H. (2021). Rapid ecosystem-scale consequences of acute deoxygenation on a Caribbean coral reef. Nat Commun 12, 4522.

Kanazawa, A., Aida, M., Yoshida, Y., Kaga, H., Katahira, T., Suzuki, L., Tamaki, S., Sato, J., Goto, H., Azuma, K., et al. (2021). Effects of synbiotic supplementation on chronic inflammation and the gut microbiota in obese patients with type 2 diabetes mellitus: a randomized controlled study. Nutrients 13, 558.

La Fata, G., Weber, P., and Mohajeri, M.H. (2018). Probiotics and the gut immune system: indirect regulation. Probiotics Antimicro Prot 10, 11–21.

Lagkouvardos, I., Overmann, J., and Clavel, T. (2017). Cultured microbes represent a substantial fraction of the human and mouse gut microbiota. Gut Microbes 8, 493–503.

Langmead, B., and Salzberg, S.L. (2012). Fast gapped-read alignment with Bowtie 2. Nat Methods 9, 357–359.

Liu, C., Du, M.X., Abuduaini, R., Yu, H.Y., Li, D.H., Wang, Y.J., Zhou, N., Jiang, M.Z., Niu, P.X., Han, S.S., et al. (2021a). Enlightening the taxonomy darkness of human gut microbiomes with a cultured biobank. Microbiome 9, 119.

Liu, C., Zhou, N., Du, M.X., Sun, Y.T., Wang, K., Wang, Y.J., Li, D.H., Yu, H.Y., Song, Y., Bai, B.B., et al. (2020). The Mouse Gut Microbial Biobank expands the coverage of cultured bacteria. Nat Commun 11, 79.

Liu, P., Zhang, T., Zheng, Y., Li, Q., Su, T., and Qi, Q. (2021b). Potential one-step strategy for PET degradation and PHB biosynthesis through co-cultivation of two engineered microorganisms. Eng Microbiol 1, 100003.

Liu, W., Fang, X., Zhou, Y., Dou, L., and Dou, T. (2022). Machine learning-based investigation of the relationship between gut microbiome and obesity status. Microbes Infect 24, 104892.

Lohia, S., Vlahou, A., and Zoidakis, J. (2022). Microbiome in chronic kidney disease (CKD): an omics perspective. Toxins 14, 176.

Macmicking, J.D. (2017). Bacteria disarm host-defence proteins. Nature 551, 303–304.

Mars, R.A.T., Yang, Y., Ward, T., Houtti, M., Priya, S., Lekatz, H.R., Tang, X., Sun, Z., Kalari, K.R., Korem, T., et al. (2020). Longitudinal multi-omics reveals subset-specific mechanisms underlying irritable bowel syndrome. Cell 183, 1137–1140.

Matchado, M.S., Lauber, M., Reitmeier, S., Kacprowski, T., Baumbach, J., Haller, D., and List, M. (2021). Network analysis methods for studying microbial communities: A mini review. Comput Struct Biotechnol J 19, 2687–2698.

Mitri, S., and Foster, K.R. (2013). The genotypic view of social interactions in microbial communities. Annu Rev Genet 47, 247–273.

Nash, A.K., Auchtung, T.A., Wong, M.C., Smith, D.P., Gesell, J.R., Ross, M.C., Stewart, C.J., Metcalf, G.A., Muzny, D.M., Gibbs, R.A., et al. (2017). The gut mycobiome of the Human Microbiome Project healthy cohort. Microbiome 5, 153.

Odamaki, T., Kato, K., Sugahara, H., Hashikura, N., Takahashi, S., Xiao, J., Abe, F., and Osawa, R. (2016). Age-related changes in gut microbiota composition from newborn to centenarian: a cross-sectional study. BMC Microbiol 16, 90.

Olm, M.R., Brown, C.T., Brooks, B., and Banfield, J.F. (2017). dRep: a tool for fast and accurate genomic comparisons that enables improved genome recovery from metagenomes through de-replication. ISME J 11, 2864–2868.

Palmer, J.D., and Foster, K.R. (2022). Bacterial species rarely work together. Science 376, 581–582.

Pan, Z., Hu, Y., Huang, Z., Han, N., Li, Y., Zhuang, X., Yin, J., Peng, H., Gao, Q., Zhang, W., et al. (2022). Alterations in gut microbiota and metabolites associated with altitude-induced cardiac hypertrophy in rats during hypobaric hypoxia challenge. Sci China Life Sci 65, 2093–2113.

Parks, D.H., Chuvochina, M., Waite, D.W., Rinke, C., Skarshewski, A., Chaumeil, P.A., and Hugenholtz, P. (2018). A standardized bacterial taxonomy based on genome phylogeny substantially revises the tree of life. Nat Biotechnol 36, 996–1004.

Peng, W., Yi, P., Yang, J., Xu, P., Wang, Y., Zhang, Z., Huang, S., Wang, Z., and Zhang, C. (2018). Association of gut microbiota composition and function with a senescence-accelerated mouse model of Alzheimer's Disease using 16S rRNA gene and metagenomic sequencing analysis. Aging 10, 4054–4065.

Petrov, V.A., Saltykova, I.V., Zhukova, I.A., Alifirova, V.M., Zhukova, N.G., Dorofeeva, Y.B., Tyakht, A.V., Kovarsky, B.A., Alekseev, D.G., Kostryukova, E.S., et al. (2017). Analysis of gut microbiota in patients with Parkinson's disease. Bull Exp Biol Med 162, 734–737.

Poyet, M., Groussin, M., Gibbons, S.M., Avila-Pacheco, J., Jiang, X., Kearney, S.M., Perrotta, A.R., Berdy, B., Zhao, S., Lieberman, T.D., et al. (2019). A library of human gut bacterial isolates paired with longitudinal multiomics data enables mechanistic microbiome research. Nat Med 25, 1442–1452.

Qian, Y., Yang, X., Xu, S., Huang, P., Li, B., Du, J., He, Y., Su, B., Xu, L.M., Wang, L., et al. (2020). Gut metagenomics-derived genes as potential biomarkers of Parkinson's disease. Brain 143, 2474–2489.

Ruaud, A., Esquivel-Elizondo, S., de la Cuesta-Zuluaga, J., Waters, J.L., Angenent, L.T., Youngblut, N.D., and Ley, R.E. (2020). Syntrophy via interspecies H$_2$ transfer between *Christensenella* and *Methanobrevibacter* underlies their global cooccurrence in the human gut. mBio 11, e03235.

Seemann, T. (2014). Prokka: rapid prokaryotic genome annotation. Bioinformatics 30, 2068–2069.

Sugihara, G., May, R., Ye, H., Hsieh, C., Deyle, E., Fogarty, M., and Munch, S. (2012). Detecting causality in complex ecosystems. Science 338, 496–500.

Uritskiy, G.V., DiRuggiero, J., and Taylor, J. (2018). MetaWRAP—a flexible pipeline for genome-resolved metagenomic data analysis. Microbiome 6, 158.

Venturelli, O.S., Carr, A.V., Fisher, G., Hsu, R.H., Lau, R., Bowen, B.P., Hromada, S., Northen, T., and Arkin, A.P. (2018). Deciphering microbial interactions in synthetic human gut microbiome communities. Mol Syst Biol 14, e8157.

Weiss, A.S., Burrichter, A.G., Durai Raj, A.C., von Strempel, A., Meng, C., Kleigrewe, K., Münch, P.C., Rössler, L., Huber, C., Eisenreich, W., et al. (2022). In vitro interaction network of a synthetic gut bacterial community. ISME J 16, 1095–1109.

Xia, L.C., Steele, J.A., Cram, J.A., Cardon, Z.G., Simmons, S.L., Vallino, J.J., Fuhrman, J.A., and Sun, F. (2011). Extended local similarity analysis (eLSA) of microbial community and other time series data with replicates. BMC Syst Biol 5, S15.

Yuan, J., Wen, T., Yang, S., Zhang, C., Zhao, M., Niu, G., Xie, P., Liu, X., Zhao, X., Shen, Q., et al. (2023). Growth substrates alter aboveground plant microbial and metabolic properties thereby influencing insect herbivore performance. Sci China Life Sci 66, 1728–1741.

Zimmermann, J., Kaleta, C., and Waschina, S. (2021). gapseq: informed prediction of bacterial metabolic pathways and reconstruction of accurate metabolic models. Genome Biol 22, 81.